Computed Relationships Between the Inherent and Apparent Optical Properties of a Flat Homogeneous Ocean

Howard R. Gordon, Otis B. Brown, and Michael M. Jacobs

Monte Carlo simulations of the transfer of radiation in the ocean are used to compute the apparent optical properties of a flat homogeneous ocean as a function of the inherent optical properties. The data are used to find general relationships between the inherent and apparent optical properties for optical depths $\tau \leq 4$. The results indicate that the apparent optical properties depend on the phase function only through the back scattering probability. It is shown that these relations can be used with measurements of the upwelling and downwelling irradiance, the beam attenuation coefficient, and the incident radiance distribution to determine the absorption coefficient, the scattering coefficient, and the backward and forward scattering probabilities.

Introduction

Very sophisticated instrumentation is required for *in situ* measurement of the fundamental or inherent optical properties of the oceans.[1] Because of this, only a relatively small number of such measurements have been carried out compared to the large number of irradiance measurements in the literature.[2] In fact, the techniques of determining in-water irradiance have been refined to the extent that a large body of spectral irradiance data is now available.[3] Unfortunately, the in-water irradiance depends strongly on the radiance distribution incident on the sea surface as well as the inherent properties of the medium and does not lend itself well to direct interpretation. Furthermore, to our knowledge, irradiance data have yet to be used to determine the inherent properties of the ocean. It is important then to understand in detail the dependence of in-water irradiances on the inherent properties and the incident radiance distribution. This is difficult to achieve experimentally, so in this paper we shall determine general relationships between the so-called apparent and inherent optical properties of flat homogeneous ocean through simulations of the solution of the radiative transfer equation.

Apparent Optical Properties

Preisendorfer[4] has defined inherent and apparent optical properties of the sea according to their invariance properties under changes in the radiance distribution about the point at which the property is measured. If the property is invariant with respect to changes in the radiance distribution, it is said to be an inherent optical property, otherwise it is an apparent optical property. Clearly the radiance distribution itself must be an apparent optical property of the ocean. In a spherical coordinate system located at the surface of a flat homogeneous ocean with z axis pointing into the water, the radiance distribution is denoted by $N(z, \theta, \phi)$. In the present work, polarization is ignored so N is a scalar function of position and direction. This is the radiance at a depth z traveling in a direction specified by polar angle θ and the azimuth angle ϕ. The radiance can be integrated over solid angle to yield the upwelling (+) and downwelling (−) irradiance $H(z, \pm)$ and scalar irradiance $h(z, \pm)$, i.e.

$$H(z, \pm) = \int_{\pm} N(z, \theta, \phi) |\cos\theta| \, d\Omega, \tag{1}$$

$$h(z, \pm) = \int_{\pm} N(z, \theta, \phi) d\Omega, \tag{2}$$

$$h(z) = h(z, +) + h(z, -),$$

where the minus sign on the integral is used to denote integration limits from 0 to $\pi/2$ for θ, and the plus sign denotes integration from $\pi/2$ to π. The above irradiance functions are of course apparent optical properties of the medium. From these irradiances, Preisendorfer has defined several other apparent properties of the medium. Some of these are:
the distribution functions

$$D(z, \pm) = h(z, \pm)/H(z, \pm); \tag{3}$$

the reflectance

The authors are with the Physics Department, Optical Physics Laboratory, and Rosenstiel School of Marine & Atmospheric Sciences, University of Miami, Coral Gables, Florida 33124.

Received 19 July 1974.

$$R(z,-) = H(z,+)/H(z,-) = 1/R(z,+); \quad (4)$$

and the irradiance attenuation coefficients

$$K(z,\pm) = -[1/H(z,\pm)](d/dz)H(z,\pm). \quad (5)$$

In the ocean optics literature, many more measurements of $H(z, \pm)$ than $h(z, \pm)$ or $N(z, \theta, \phi)$ appear to have been carried out.[3] This is of course due to the greater difficulty encountered in constructing instrumentation for measurement of the latter quantities [especially $N(z, \theta, \phi)$]. Moreover, commercial instruments are available for measuring $H(z, \pm)$. Clearly measurement of $N(z, \theta, \phi)$ allows computation of all the above apparent optical properties.

Inherent Optical Properties

The inherent optical properties of the medium are the absorption coefficient a, the scattering coefficient b, the attenuation coefficient c, and the volume scattering function $\beta(\theta)$. If a beam of parallel light of irradiance H_0 (measured normal to the beam) is passed through a slab of the medium of thickness Δr, then[2] a, b, and c are, respectively, the fraction of radiant power removed from the beam, respectively, by absorption, scattering, and scattering plus absorption, divided by Δr $(c = a + b)$. If the above beam has a cross sectional area A and an intensity $\Delta J(\theta)$ is observed to be scattered in a direction θ from the incident beam by the volume $A\Delta r$, the volume scattering function $\beta(\theta)$ is defined according to

$$\beta(\theta) \equiv [\Delta J(\theta)]/(H_0 A \Delta r). \quad (6)$$

$\beta(\theta)$ is related to b through

$$b = 2\pi \int_0^\pi \beta(\theta) \sin\theta d\theta. \quad (7)$$

Implicit in these definitions is the fact that the incident beam be monochromatic or at most be composed of a band wavelengths very small compared to the visible spectrum. A further requirement is of course that $c\Delta r \ll 1$ and the largest linear dimension of A be much smaller than $1/c$.

It is very difficult to measure these inherent optical properties of the ocean and even pure water, as has been pointed out by Tyler *et al.*[5] The problem is that $\beta(\theta)$ is so strongly peaked in the forward direction that Eq. (7) can lead to values of b that are far too small unless accurate measurements of $\beta(\theta)$ can be made near $\theta = 0°$; c is likewise difficult to measure since some small angle of scattered light will inevitably reach the sensor yielding an attenuation that is again too small. Although there are commercial c meters available, they probably do not measure c as accurately as the commercial irradiance meters measure $K(z, \pm)$. a can be approximately measured by collecting the forward scattered light and using $\beta(\theta)$ at larger angles to correct the result. However, in this case not all the photons traverse the same pathlength in the medium so an error is still unavoidable. Only recently Petzold[1] has reported the development of several instruments that minimize these problems, and the prospects for quality measurements of a, b, c, and $\beta(\theta)$ at selected wavelengths are good.

Radiative Transfer Equation

The inherent and apparent optical properties are related through the radiative transfer equation,

$$\left[\mu\frac{d}{dz} + c(z)\right] N(z,\theta,\phi) = b(z)\int_{\Omega'} P(z;\theta,\phi;\theta',\phi')N(z,\theta',\phi')d\Omega', \quad (8)$$

where $\mu = \cos\theta$,

$$P(z;\theta,\phi;\theta',\phi') = \beta(z,\theta,\phi,\theta',\phi')/b(z) \quad (9)$$

is the phase function for scattering from a direction (θ', ϕ') to (θ, ϕ) at a depth z, and the integration is to be carried out over all Ω'. In the ocean case, this equation is subject to the boundary condition at $z = 0$ that the downward radiance be composed of that refracted into the water through the interface plus the upward radiance that is reflected back into the medium by the interface according to the Fresnel reflection law for unpolarized radiation. If the optical depth defined by

$$\tau = \int_0^z c(z)dz$$

is taken as the independent variable, the equation reduces to

$$\left(\mu\frac{d}{d\tau} + 1\right) N(\tau,\theta,\phi) = \omega_0(\tau)\int_{\Omega'} P(\tau,\theta,\phi;\theta',\phi')N(\tau,\theta',\phi')d\Omega', \quad (10)$$

indicating that $N(\tau, \theta, \phi)$ is completely determined by ω_0, P, and the incident radiance distribution. In this representation, all the inherent optical properties become functions of τ instead of z, and Eq. (5) becomes

$$\frac{K(\tau,\pm)}{c} = -\frac{1}{H(\tau,\pm)}\frac{d}{d\tau}H(\tau,\pm). \quad (11)$$

The purpose of this work is to demonstrate through simulations of the solution of Eq. (10) that some of the apparent optical properties of the ocean, in particular $K(\tau, \pm)$ and $R(\tau, -)$, can be written in a simple manner in terms of the inherent optical properties, and that these apparent properties when combined with c can be used to determine a and b if the form of the radiance distribution incident on the sea surface is known. To this end, it is important to discuss some results of a simple quasi-single-scattering approximation that will serve as a guide in the analysis of the Monte Carlo computations discussed below.

The quasi-single-scattering approximation[6] is based on the fact that the scattering phase function is strongly peaked in the forward direction. The approximation consists of forcing photons that are not backscattered from the incident beam toward the surface to be scattered at 0° relative to the incident beam (perfect forward scattering) and hence remain

in the beam. Let the incident irradiance consist of a beam making an angle (in the water) θ_0 with respect to the inward normal. Then, since the only loss of irradiance from the incident beam is through absorption or backscattering, the irradiance attenuation coefficient becomes

$$K(\tau,-) = \{a + b[1 - F(\mu_0)]\}/\mu_0 = c[1 - \omega_0 F(\mu_0)]/\mu_0, \quad (12)$$

where $\mu_0 = \cos\theta_0$ (Ref. 7), and

$$F(\mu_0) = 1 - \left[\int_0^{2\pi}\int_0^1 P(\delta)d\mu d\phi/2\pi \int_{-1}^1 P(\mu)d\mu\right],$$

with

$$\cos\delta = -\mu\mu_0 + (1 - \mu_0^2)^{1/2}(1 - \mu^2)^{1/2}\cos(\phi).$$

$F(\mu_0)$ is the fraction of scattered light from an optically thin volume element that is not scattered toward the surface. $F(1) = F$ is the probability of single scattering through angles between 0 and 90°. Since $F(\mu_0)$ is a very weak function of μ_0 for most oceanic scattering functions, we shall replace it by F. To the same order of approximation the reflectance function just beneath the surface is found to be

$$R(0,-) = \frac{\omega_0}{1 - \omega_0 F}\int_0^{2\pi}\int_0^1 \frac{P(\delta)\mu d\mu d\phi}{\mu + \mu_0}. \quad (13)$$

The distribution functions just beneath the surface can also be computed in this approximation. For this we need only recognize that the downward irradiance and scalar irradiance consist of those incident plus the contribution due to upwelling radiance internally reflected back into the medium from the surface. With this in mind, it is easy to show that again just beneath the sea surface,

$$D(0,-) = \frac{1}{\mu_0} + \frac{1}{\mu_0^2}\frac{\omega_0}{1 - \omega_0 F}\int_0^{2\pi}\int_0^1 r(\mu, \mu') \times \left(\frac{\mu_0 - \mu}{\mu_0 + \mu}\right)P(\delta)d\mu d\phi + \ldots, \quad (14)$$

where $r(\mu, \mu')$ is the Fresnel reflectance (water to air) of the interface, and μ' is related to μ through Snell's law. The upwelling distribution function found by this method is to lowest order independent of both ω_0 and F, i.e.,

$$D(0,+) = \int_0^1 \frac{P(-\mu)}{\mu_0 + \mu}d\mu \Big/ \int_0^1 \frac{P(-\mu)\mu}{\mu_0 + \mu}d\mu. \quad (15)$$

Since the quasi-single-scattering approximation reproduces Monte Carlo calculations of the diffuse reflectance of the ocean to better than ½% for $\omega_0 \leq 0.7$, it is reasonable that for small ω_0 the appoximation should be quite good in the medium near the surface. At least we expect Eqs. (12)–(15) to provide the correct functional dependence of the apparent optical properties on the inherent optical properties. The range of validity of the quasi-single-scattering approximation is examined in Appendix A.

Calculations

We have simulated the solution of Eq. (10) by a Monte Carlo technique described earlier[8] for a flat homogeneous ocean. The scattering phase function for ocean water is the sum of the Rayleigh scattering of the water itself and scattering by suspended particles in the water. Since the particle scattering is very large in the forward direction, the shape of the phase function for the medium will depend strongly on the concentration and type of particulate matter present in the water. The present study is concerned mostly with clear ocean waters, and hence phase functions for these waters are used. It should be remembered, however, that these phase functions may also be applicable to more turbid water as well.

Input Parameters

A total of eight phase functions has been used in the simulations. These are given in Table I. Phase functions *KA, KB,* and *KC* are derived from Kullenberg's[9] measurements of $\beta(\theta)$ at 655 nm *(KA)* and 460 nm *(KC)* in the Sargasso Sea. *KB* is the average of *KA* and *KC*. Phase functions *PA* and *PB* are taken from Petzold[1] and correspond to filtered fresh water and sea water, respectively, at 530 nm. Phase functions *A, B,* and *C* are similar to *KA, KB,* and *KC;* however, they show considerably more scattering around $\theta = 180°$. *PB* exhibits the least amount of forward scattering of the above phase functions and probably represents the lower limit of forward scattering one might expect in natural waters. The backscattering probability $B = 1 - F$ is also given in Table I. We shall see below that most of the apparent optical properties of the ocean depend on the phase function through the backscattering probability alone and are therefore weak functions of the shape of $P(\theta)$. Hence, the calculations reported here will be applicable to all clear natural waters. For completeness, the computations have also been carried out for the Rayleigh phase function labeled *R,* which would be applicable to ocean water completely uncontaminated by particulate matter. The Rayleigh phase function results are discussed separately in Appendix B.

The range of ω_0 is from 0 (no scattering) to 1 (no absorption), and in this study ω_0 is varied from 0 to 0.95. In clear ocean water ω_0 probably never exceeds 0.7, however larger values have been observed[1] in turbid coastal waters.

With ω_0 and $P(\theta)$ fixed, the apparent optical properties depend only on the radiance distribution incident upon the sea surface. Since the present work is centered on transfer in the ocean, the atmosphere has not been modeled, instead most of the computations have been carried out for collimated irradiance incident on the sea surface from the zenith. This is chosen to represent the influence of direct sunlight and is henceforth referred to as the sun case. To estimate the influence of skylight on the transfer of radiation we have used an incident distribution of completely diffuse irradiance to simulate the skylight,

Table I. Phase Functions ($\times 10^2$)

θ(deg)	KA	KB	KC	A	B	C	PA	PB
1	4916	4577	4285	2630	2490	2360	3972	1662
5	574	534	500	710	678	634	407	271
10	169	158	148	201	182	168	130	131
20	29.5	29.4	29.2	52.3	46.2	42.1	34.4	54.9
30	12.6	12.0	11.4	15.8	15.6	15.4	12.2	13.3
45	3.06	3.66	4.19	4.20	4.82	5.51	4.17	5.30
60	1.09	1.58	2.00	1.47	1.94	2.36	2.37	3.09
75	0.546	0.915	1.19	0.655	1.02	1.32	1.81	2.37
90	0.344	0.661	0.952	0.383	0.708	0.998	1.56	1.95
105	0.311	0.641	0.928	0.318	0.648	0.933	1.57	1.90
120	0.317	0.732	1.09	0.324	0.717	1.05	1.76	2.08
135	0.410	0.829	1.31	0.395	0.871	1.31	2.02	2.53
150	0.492	1.02	1.62	0.542	1.16	1.71	2.29	2.97
165	0.579	1.26	1.86	0.735	1.60	2.36	3.04	3.56
170	0.595	1.31	1.93	0.795	1.91	2.71	3.43	4.15
175	0.610	1.34	1.97	1.17	2.61	4.00	3.55	4.30
180	0.617	1.36	2.00	2.04	4.30	6.31	3.66	4.45
B	0.0236	0.0506	0.0746	0.0257	0.0544	0.0799	0.1193	0.1462

and these computations are referred to as the sky case. The sky computations have been carried out only for phase functions A, B, and C. Finally several cases have been studied for phase function B in which the incident irradiance is collimated but not directed from the zenith, i.e., not normal to the sea surface. We shall find that the above set of computations is sufficient to understand the influence of the incident radiance distribution on the apparent optical properties.

The calculations using the phase functions, ω_0's, and incident radiance distributions described above have been carried out for a flat homogeneous ocean. Detectors have been placed at twenty optical depths in the medium (at depths $\tau \leq 10$) to measure $H(\tau, +)$, $H(\tau, -)$, $h(\tau, +)$, and $h(\tau, -)$. The upwelling radiance distributions just below and just above the sea surface are detected as well.

Accuracy of the Simulations

Before discussing the results of the computations it is important to insure that the computer code is capable of yielding accurate results. This has been effected by carrying out computations for a Rayleigh scattering atmosphere illuminated by collimated irradiance from the zenith. This is the same as the R-sun case, but the ocean's refractive index is charged from 1.33 to 1.00. Plass *et al.*[10] (PKB) have presented a very accurate solution for these cases using the powerful Matrix Operator method[11] with a Runge-Kutta starting point. In order to compare our computations with their's, we have placed our irradiance counters at the optical depths given in their paper. We find that the Monte Carlo (MC) and Matrix Operator (MO) calculations of $H(\tau, -)$ agree exceptionally well for all values of ω_0 for $\tau \leq 9$, which leads us to believe that our $H(\tau, -)$ computations are very accurate. Comparison of the computations of $R(\tau, -)$ for $\omega_0 = 0.1$ and 0.5 is presented in Table II showing that $R(\tau, -)$ and hence $H(\tau, +)$ become increasingly inaccurate as τ increases, especially for the small values of ω_0 due to the small number of photons contributing to $H(\tau, +)$ at great optical depth. We estimated the depth to which the accuracy of upwelling quantities is good enough to be trusted by noting at what depth our $R(\tau, -)$ departed from the smooth curve resulting from the PKB computations. For $\omega_0 = 0.1$, $R(\tau, -)$ agrees with PKB for $\tau \leq 3$, while for $\omega_0 = 0.5$ the agreement is preserved for $\tau \leq 4$, and the $\omega_0 = 0.9$ computations appear to be valid even for $\tau = 9$. This convinces us that our code is capable of accurately computing the upwelling apparent optical properties of the medium at least to $\tau = 3$ and usually to $\tau \approx 4$ using the Rayleigh phase function.

Unfortunately, we cannot test by comparison the code for phase functions showing the very pronounced forward scattering observed in sea water, since to our knowledge highly accurate interior radiances for these cases are unavailable. We can however check that our simulations satisfy an integral of the transfer equation which results when Eq. (10) is integrated over Ω; namely,[4]

Table II. Comparison Between Matrix Operator (MO) and Monte Carlo (MC) Calculations of $R(\tau,-)$ for a Rayleigh Scattering Atmosphere

	$\omega_0 = 0.1$		$\omega_0 = 0.5$	
τ	MO	MC ($\times 10^2$)	MO	MC ($\times 10$)
0	1.777	1.783	1.207	1.215
0.4795	1.785	1.799	1.241	1.251
0.9795	1.790	1.799	1.258	1.263
2.98	1.797	1.792	1.289	1.289
8.98	1.802	1.364	1.311	1.491

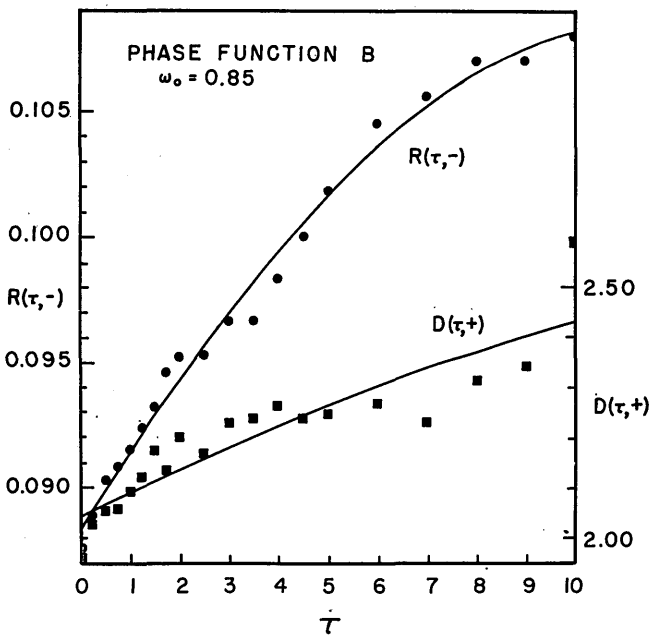

Fig. 1. Comparison between the direct Monte Carlo simulation results for $R(\tau, -)$ and $D(\tau, +)$ (data points) with those determined from irradiances fit to Eq. (17) (smooth curves.)

$$1 - \omega_0(\tau) = \frac{1}{h(\tau)} \frac{d}{d\tau}[H(\tau, +) - H(\tau, -)]. \quad (16)$$

Using all the data for each ω_0 and phase function, to compute $1 - \omega_0$, the mean difference between the computed value and the actual value of this quantity is usually 1.5% indicating the simulations satisfy energy conservation in the presence of absorption to this accuracy.

We shall assume in what follows that any observable dependent on upwelling photons is accurate for $\tau \leq 4$, and other observables [such as $H(\tau, -)$] are accurate to $\tau = 10$.

Removal of Statistical Fluctuations

Because all Monte Carlo calculations contain statistical fluctuations, we have treated the computations as raw experimental data that must be smoothed before accurate values for quantities such as $K(\tau, \pm)$, $R(\tau, \pm)$, and $D(\tau, \pm)$ can be derived. The irradiances decay approximately in an exponential fashion with depth, so we have fit them by least squares to

$$I = \exp[-(c_0 + c_1\tau + c_2\tau^2)], \quad (17)$$

where I is any of the four irradiances in Eqs. (1) and (2). It is found that the agreement between these calculated irradiances from Eq. (17) and the observed irradiances (or raw data) are excellent, and the calculated irradiances are now free of statistical fluctuations.

To see how the computations in Eq. (17) reproduce the apparent optical properties $R(\tau, -)$ and $D(\tau, +)$ as a function of depth, Fig. 1 compares the computed values given by Eq. (17) with the original Monte Carlo calculations for phase function B with $\omega_0 = 0.85$. It is seen that the computed and observed (Monte Carlo) $R(\tau, -)$ are in good agreement, while there is considerable scatter in the $D(\tau, +)$ for large τ data. For typical values of $R(\tau, -)$, the upwelling irradiances are about 1 or 2 orders of magnitude less accurate than the downwelling irradiances. So ranked in order of their accuracy, we have $K(\tau, -)$, $D(\tau, -)$, $K(\tau, +)$, $R(\tau, -)$, and $D(\tau, +)$, i.e., $K(\tau, -)$ is the most accurate property, and $D(\tau, +)$ (the ratio of two upwelling quantities) is the least accurate. It is not surprising then that considerable scatter is observed in the $D(\tau, +)$ data. Since the computations are more accurate for small τ, we have fit the computations to Eq. (17) using data for the first seven values as well as all twenty values of τ. The results presented below for $\tau = 0$ and 1 are derived from the fits for the first seven values of τ, while all other results are from the entire set of twenty τ values.

Analysis of the Results

Downwelling Irradiance Attenuation Coefficient

Figures 2 and 3 (left panels) show the irradiance attenuation coefficient $K(0, -)/c$ just beneath the sea

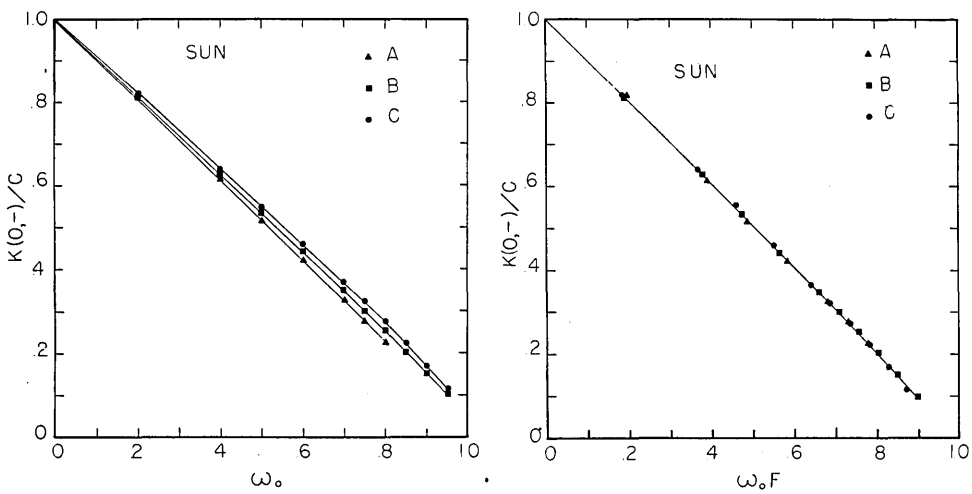

Fig. 2. Dependence of $K(0, -)/c$ on ω_0 and F for phase functions A, B, and C in the sun case.

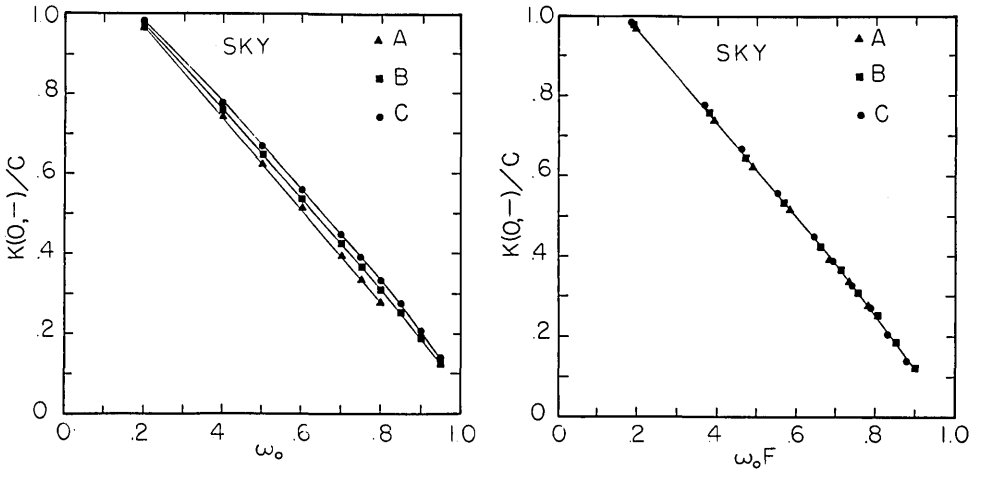

Fig. 3. Dependence of $K(0, -)/c$ on ω_0 and F for phase functions A, B, and C in the sky case.

Table III. Variation in $K(\tau,-)/cD_0$ with the Incident Radiance Distribution for $\tau = 1.50$ and Phase Function B

$\theta_0 w$	$\omega_0 = 0.2$	$\omega_0 = 0.4$	$\omega_0 = 0.6$	$\omega_0 = 0.8$
0°	0.8307	0.6551	0.4704	0.2754
10°	0.8303	0.6549	0.4707	0.2762
20°	0.8323	0.6555	0.4707	0.2767
30°	0.8304	0.6538	0.4772	0.2803
40°	0.8330	0.6543	0.4779	0.2841
Sky	0.8253	0.6555	0.4784	0.2853

surface for the sun and sky cases, respectively, as a function of ω_0 and the phase function. The general shape of the $K(\tau, -)/c$, ω_0 relationship is similar to that found by Prieur and Morel[12] for the near-asymptotic light field and Beardsley and Zaneveld[13] for the asymptotic field. Equation (12) suggests that the influence of the phase function can be removed from $K(\tau, -)/c$ by plotting this quantity as a function of $\omega_0 F$ rather than just ω_0. The right panels of Figs. 2 and 3 give $K(0, -)/c$ as a function of $\omega_0 F$ which shows that the results for the three phase functions all fall on the same smooth curve for both the sun and sky cases. Figure 4 confirms that this simplification occurs in $K(\tau, -)/c$ down to at least $\tau = 4$. The main difference between the sun and sky cases is that the slope and intercept of the $K(\tau, -)/c$ vs $\omega_0 F$ relationship are both larger in the sky case. Preisendorfer[4] has shown that for $\omega_0 = 0$, $K(\tau, -)/c = D(\tau, -)$ independent of the form of the incident radiance distribution. For collimated incident irradiance $D(\tau, -)$ at $\omega_0 = 0$ is $1/\mu_0$, and Eq. (12) becomes

$$K(\tau,-)/[cD_0(\tau,-)] = 1 - \omega_0 F, \qquad (12')$$

where $D_0(\tau, -)$ is the value of $D(\tau, -)$ at $\omega_0 = 0$. Equation (12′) then suggests that $K(\tau, -)/cD_0(\tau, -)$ may depend only on $\omega_0 F$ and not even on the form of the incident radiance distribution. The validity of this is demonstrated in Table III in which $K(\tau, -)/cD_0(\tau, -)$ at $\tau = 1.50$ is given for collimated incident irradiance making an angle θ_0 with the inward normal to the sea surface and a sky of uniform radiance. Since the maximum value of θ_0 is 48.6°, it is clear that to very good accuracy $K(\tau, -)/cD_0(\tau, -)$ is independent of the incident radiance distribution and hence might be called a quasi-inherent optical property of the medium. $D_0(\tau, -)$ can be computed if the incident radiance distribution $N(\mu, \phi)$ is known and is in general given by

$$D_0(\tau,-) = \int_0^{2\pi}\int_0^1 N(\mu,\phi)T(\mu,\mu') \times \exp(-\tau/\mu')d\mu' d\phi \Big/ \int_0^{2\pi}\int_0^1 N(\mu,\phi)T(\mu,\mu')\mu' \times \exp(-\tau/\mu')d\mu' d\phi, \qquad (18)$$

where $T(\mu, \mu')$ is the Fresnel transmittance of the interface (air to water), and μ and μ' are related by Snell's law.

Since the curves in Figs. 2, 3, and 4 are smooth and nearly linear, it is possible to derive an analytic expression for $K(\tau, -)/cD_0(\tau, -)$ of the form

$$K(\tau,-)/cD_0(\tau,-) = \sum_{n=0}^{N} k_n(\tau)(\omega_0 F)^n \qquad (19)$$

by least squares. It is also useful to invert the above equation to yield

$$\omega_0 F = \sum_{n=0}^{N} k_n'(\tau)[K(\tau,-)/cD_0(\tau,-)]^n. \qquad (19')$$

The coefficients k_n and k_n' for $N = 3$ are given in Table IV for $\tau = 0$ to 4. With these coefficients, Eq. (19) reproduces $K(\tau, -)/cD_0(\tau, -)$ with a mean error of about 3%.

If $D_0(\tau, -)$ or equivalently the radiance distribution incident on the sea surface is known, Eq. (19′) can be used with measurements of $K(\tau, -)$ and c to determine $\omega_0 F$. Furthermore in most natural waters, $F \approx 0.95$ to 0.98, so $\omega_0 F \approx \omega_0$, and Eq. (19) gives a good estimate of ω_0. Although the calculations have been carried out only for a flat ocean, Eqs. (19) and (19′) can be used for a rough surface, because the surface shape will only influence $D_0(\tau, -)$, i.e., the ra-

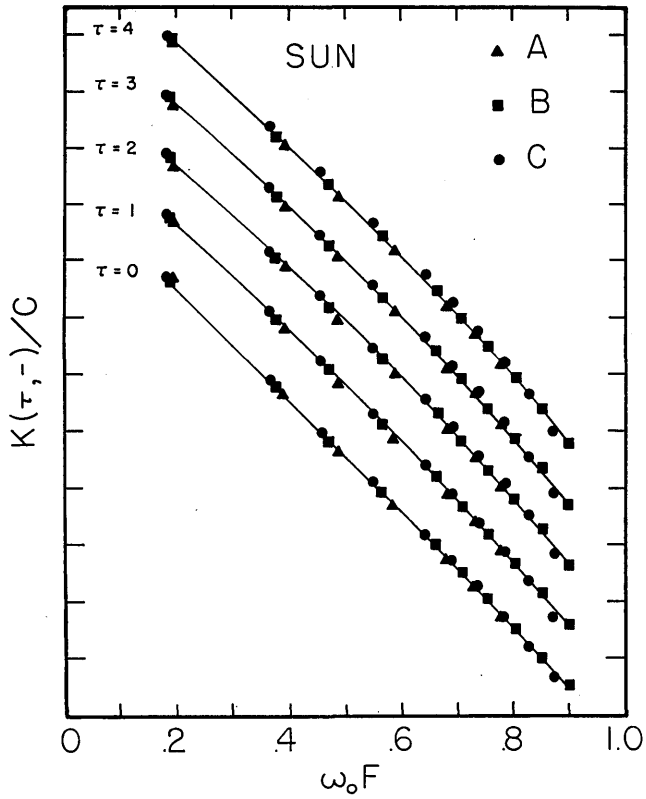

Fig. 4. Dependence of $K(\tau, -)/c$ on $\omega_0 F$ and τ for phase functions A, B, and C in the sun case. Each successive τ curve has been shifted upward one unit to facilitate presentation.

for three different phase functions A, B, and C fall on a single smooth curve. Figure 6 indicates that this is also valid when the in-water reflection function $R(\tau, -)$ is plotted against X for $\tau = 0$, 2, and 4 again for the sun case. Similar results are obtained for R_d and $R(\tau, -)$ when the sky case is considered.

As with $K(\tau, -)/cD_0(\tau, -)$, Figs. 5 and 6 suggest $R(\tau, -)$ can be represented by the simple expression

$$R(\tau, -) = \sum_{n=0}^{N} r_n(\tau) X^n, \tag{20}$$

or that X can be determined from $R(\tau, -)$ through

$$X = \sum_{n=0}^{N} r_n'(\tau)[R(\tau, -)]^n. \tag{20'}$$

Unfortunately, we see from Table V that in contrast to $K(\tau, -)/cD_0(\tau, -)$, $R(\tau, -)$ is a slowly increasing function of θ_0 and weakly dependent on the form of the incident radiance distribution. It is not possible then to derive a single set of coefficients r_n and r_n' that will be valid for all incident distributions. Because of this, we have computed these coefficients for the sun case ($\theta_0 = 0$) and the sky case separately. These are presented in Table VI in which the upper number for each τ refers to the sun case and the lower number the sky case. Equation (20) reproduces $R(\tau, -)$ with a mean error of about 2%. From Table V we see that the sun coefficients should be used for $\theta_0 \leq 20°$, while the sky coefficients are more suitable if $\theta_0 \gtrsim 30°$.

Table IV. Expansion Coefficients for Eqs. (19) and (19')

τ	k_0	k_1	k_2	k_3	k_0'	k_1'	k_2'	k_3'
0	1.0016	−0.9959	0.1089	−0.1527	0.9588	−0.7408	−0.3935	0.1776
1	0.9999	−0.9221	0.0522	−0.1584	0.9690	−0.7124	−0.3870	0.1303
2	0.9999	−0.9259	0.1749	−0.2780	0.9673	−0.6148	−0.5520	0.1988
3	0.9999	−0.8956	0.1526	−0.2838	0.9683	−0.5926	−0.5536	0.1772
4	0.9999	−0.8653	0.1305	−0.2897	0.9695	−0.5737	−0.5465	0.1501

diance distribution just beneath the sea surface. $D_0(\tau, -)$ can be computed from the surface slope distribution of Cox and Munk[14] if the surface wind speed is known.

Reflection Function

Equation (13) shows that $R(0, -)$ is proportional to $\omega_0/(1 - \omega_0 F)$; however, noting that the integral in Eq. (13) will be roughly proportional to the backscattering probability B, it is reasonable to expect that the reflection functions should be proportional to

$$X = \omega_0 B/(1 - \omega_0 F).$$

This is verified for the diffuse reflectance R_d [$= R(0, -)$ measured just above the sea surface] in Fig. 5, which for the sun case indicates that when the reflectance is plotted against X rather than ω_0, the results

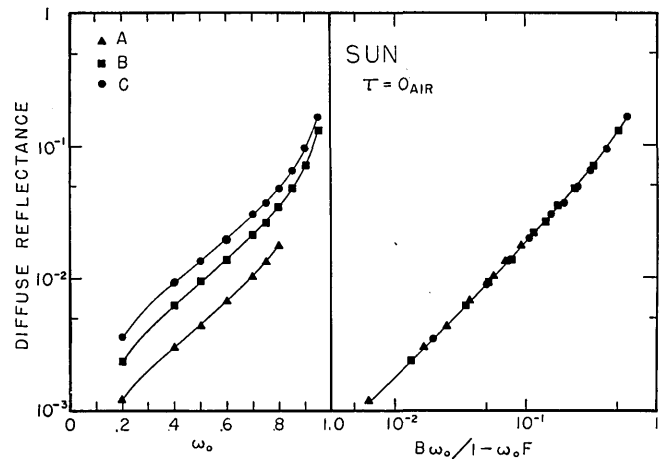

Fig. 5. Dependence of the diffuse reflectance of the ocean on ω_0 and the parameter $X = \omega_0 B/(1 - \omega_0 F)$ for phase functions A, B, and C in the sun case.

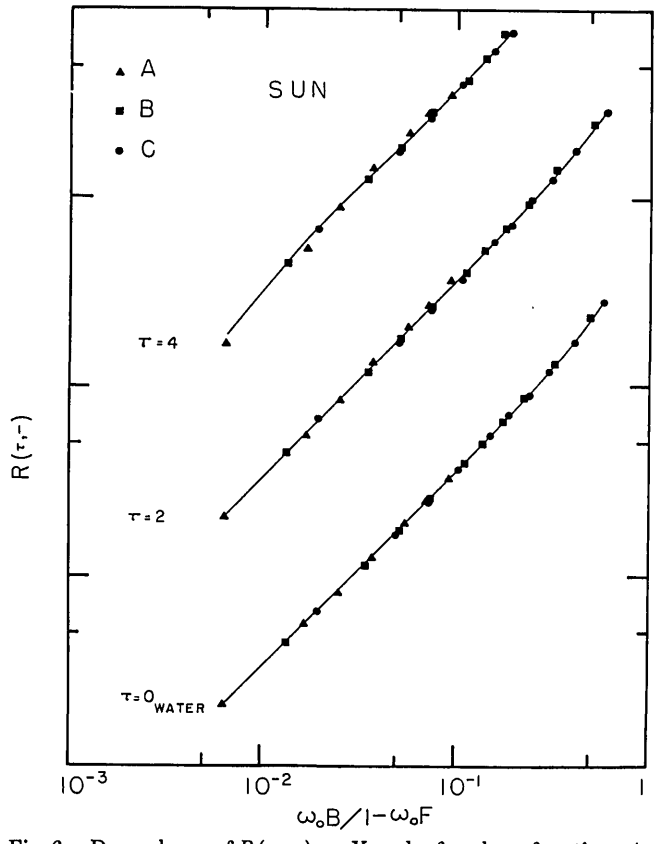

Fig. 6. Dependence of $R(\tau, -)$ on X and τ for phase functions A, B, and C in the sun case. Each successive τ curve has been shifted upward 1 order of magnitude to facilitate presentation.

Table V. Variation in $R(\tau,-)$ with the Incident Radiance Distribution for $\tau = 1.50$ and Phase Function B

θ_0	$\omega_0 = 0.2$	$\omega_0 = 0.4$	$\omega_0 = 0.6$	$\omega_0 = 0.8$
0°	0.00458	0.01191	0.02655	0.06910
10°	0.00455	0.01169	0.02675	0.06962
20°	0.00461	0.01227	0.02736	0.07211
30°	0.00467	0.01306	0.02972	0.07673
40°	0.00520	0.01429	0.0327	0.08264
Sky	0.00485	0.01322	0.02987	0.07575

Distribution Functions $D(\tau, \pm)$

Equation (14) suggests that the dependence of $D(\tau, -)$ on the phase function can be accounted for in a way similar to that of $R(\tau, -)$ with the parameter X. We have also found this to be valid, which implies that $D(\tau, -)$ can be expanded in terms of X in a manner similar to $R(\tau, -)$,

$$D(\tau,-) - D_0(\tau,-) = \sum_{n=0}^{N} d_n(\tau)X^n. \tag{21}$$

Table VII shows that the variation of $D(\tau, -) - D_0(\tau, -)$ with the incident radiance distribution is similar to that of $R(\tau, -)$, and so the coefficients in Eq. (21) must be determined for the sun and sky cases separately. These coefficients are given in Table VIII. The mean error in Eq. (21) is about 7% if it is not used for $\omega_0 \leq 0.4$ for the sky case. As with $R(\tau, -)$, Table VII indicates the sun coefficients should be used for $\theta_0 \leq 20°$ and the sky coefficients for $\theta_0 \gtrsim 30°$.

The upwelling distribution function $D(\tau, +)$ being the ratio of two upwelling quantities is not given to sufficient accuracy by our code to merit analysis. However, Eq. (15) implies that $D(0, +)$ should be nearly independent of ω_0, and this will be verified in Appendix A.

Applications

We feel that the major value and potential application of this work stems from the possibility of using Eqs. (19′) and (20′) to determine the inherent optical properties of homogeneous oceans from measurement of c and $H(z \pm)$ alone. This is accomplished by finding $\omega_0 F$ with Eq. (19′) from which ω_0 and hence F and B can be determined using Eq. (20′). Thus a, b, F, and B can be deduced through experimental measurements of c and $H(z, \pm)$ once the form of the incident radiance distribution is known [for computation of $D_0(\tau, -)$].

We will now present two examples to assess the accuracy to which this can be accomplished. The first example consists of a numerical experiment in which a phase function given by Petzold for the Tongue of

Table VI. Expansion Coefficients for Eqs. (20) and (20′) for the Sun and Sky Cases

τ	r_0	r_1	r_2	r_3	r_0'	r_1'	r_2'	r_3'
0	0.0001	0.3244	0.1425	0.1308	−0.0003	3.0770	−4.2158	3.5012
	0.0003	0.3687	0.1802	0.0740	−0.0008	2.6987	−3.2310	2.8947
1	0.0000	0.3355	0.1564	0.1233	0.0002	2.9592	−3.9051	3.1737
	0.0005	0.3741	0.2353	−0.0037	−0.0008	2.6204	−3.2048	3.2993
2	−0.0002	0.3502	0.1202	0.1730	0.0004	2.8809	−3.5590	2.5424
	0.0004	0.3826	0.2229	0.0081	−0.0005	2.5650	−2.9298	2.8087
3	−0.0003	0.3589	0.1184	0.1796	0.0007	2.8131	−3.3566	2.2948
	0.0004	0.3874	0.2274	0.0017	−0.0003	2.5262	−2.8074	2.6296
4	−0.0004	0.3668	0.1177	0.1820	0.0010	2.7524	−3.1727	2.0866
	0.0004	0.3892	0.2382	−0.0096	−0.0003	2.5054	−2.7901	2.6772

Table VII. Variation in $D(\tau,-) - D_0(\tau,-)$ with the Incident Radiance Distribution for $\tau = 1.50$ and Phase Function B

$\theta_0 w$	$\omega_0 = 0.2$	$\omega_0 = 0.4$	$\omega_0 = 0.6$	$\omega_0 = 0.8$
0°	0.0218	0.0504	0.0879	0.1548
10°	0.0208	0.0497	0.0875	0.1483
20°	0.0215	0.0545	0.0952	0.1677
30°	0.0228	0.0582	0.1014	0.1870
40°	0.0241	0.0599	0.1117	0.2008
Sky	0.0274	0.0589	0.1105	0.1927

Table VIII. Expansion Coefficients in Eqs. (21) for the Sun and Sky Cases

τ	d_0	d_1	d_2	d_3
0	0.0002	0.2991	0.1492	0.3115
	−0.0037	0.3664	0.1689	0.0131
1	0.0058	0.8432	−1.1932	1.1765
	0.0112	1.2491	−2.4523	2.4076
2	0.0123	1.0381	−1.3613	1.2780
	0.0171	1.5103	−2.9670	2.7573
3	0.0174	1.2921	−1.7987	1.5510
	0.0238	1.8187	−3.6898	3.3283
4	0.0220	1.5151	−2.1851	1.7876
	−0.003	2.5054	−2.7901	2.6772

Table IX. Test of Scheme for Finding ω_0 and B

τ	ω_0	B
0	0.499	0.0235
1	0.512	0.0197
2	0.520	0.0209
3	0.523	0.0206
4	0.526	0.0207
True	0.500	0.0253

the Ocean (AUTEC Station 7) in the Bahamas was used along with $c = 1$ and $\omega_0 = 0.5$ to compute the experimental values of $H(z, \pm)$ with collimated incident irradiance from the zenith. The experimental values were then fit to Eq. (17) to remove some of the statistical fluctuations before computation of $K(\tau, -)/c$ and $R(\tau, -)$. These functions were then used with Eqs. (19′) and (20′) to compute ω_0 and B as a function of τ [note that $D_0(\tau, -) = 1$ in this example]. The results of this exercise are shown in Table IX where the computed values of ω_0 and B are compared with the true values. We see that the computed value of ω_0 agrees well with the true value for small τ, while for larger τ the error in ω_0 becomes of the order of 5%. Likewise, the computed value of B is most accurate at $\tau = 0$, and as τ increases the error in this quantity is about 20%. On this basis we expect to be able to determine ω_0 and B from Eqs. (19′) and (20′) with errors of at most 5% in ω_0 and 20% in B.

As a second example of applying the equations developed here, we have used data given by Preisendorfer[4] from Lake Pend Oreille, Idaho together with Eqs. (19′) and (20′) to again find ω_0 and B. In this case $c = 0.402$ m^{-1}, and the smallest depth for which complete data are given is 10.4 m ($\tau = 4.18$) so the equations for $\tau = 4$ have been used. Also, sky light was ignored, so $D_0(\tau, -) = 1/\cos\theta_0$ or 1.0979 in Eq. (19′). The resulting ω_0 was 0.728 compared to the measured value of 0.714, and the value of B was found to be 0.0227. Unfortunately B was not measured experimentally. $D(\tau, -)$ was found by averaging the results of computations using the sun and sky equations, since Table VII shows that for the given θ_0 (~25°), $D(\tau, -) - D_0(\tau, -)$ is roughly this average for large ω_0. The resulting $D(\tau, -)$ was 1.191 compared to the experimental value of 1.288. The agreement between the experimental and computed values of ω_0 is certainly striking and demonstrates the potential value of the relationships developed here. The fact that the computed $D(\tau, -)$ differs considerably from the experimental value could be in part due to the assumption of negligible sky light in the incident irradiance. The ability of these techniques to provide reasonable estimates of B is very important since the diffuse reflectance of the ocean, which is important in remote sensing work, is directly proportional to B. This quantity is very difficult to measure directly without the sophisticated instrumentation described by Petzold, and we feel the estimate provided by the above technique is probably at least as good as experimental measurements of this quantity.

Even if c is not measured, it is possible to use Eqs. (20′) and (21) to estimate the absorption ceofficient a from $H(z, \pm)$ measurements with Preisendorfer's equation[4]

$$a = \frac{K(z,-) - R(z,-)K(z,+)}{D(z,-) + R(z,-)D(z,+)}. \tag{22}$$

$H(z, \pm)$ measurements give $R(z, -)$ and $K(z, \pm)$ so only $D(z, -)$ and $D(z, +)$ need to be determined. If we assume $D(z, +)/D(z, -) \approx 2$ as the present calculations show, Eq. (22) for Lake Pend Oreille becomes

$$a = 0.1446 \text{ m}^{-1}/D(\tau, -),$$

where τ is unknown. Using $R(z, -)$ with Eq. (20′) to find X for each τ, these X's can be inserted into Eq. (21) to find five values of $D(\tau, -)$. These give a = 0.130, 0.125, 0.123, 0.121, and 0.121 m^{-1} for $\tau = 0$, 1, 2, 3, and 4, respectively, compared to the experimental value of 0.115. Hence in this example a could be found to within about 15% without using c. Beardsly and Zaneveld[13] have also established this for the near-asymptotic case.

Finally, of course, the relationships developed here can be used to compute the apparent optical properties from the inherent optical properties. This has been done by Maul and Gordon[15] in their computations of the diffuse reflectance spectrum of the oceans as a function of the concentration of suspended material and yellow substances for remote sensing purposes. Furthermore, the effective radiation penetration depth[16] $[1/K(0, -)]$ can also be computed as a function of the oceanic properties.

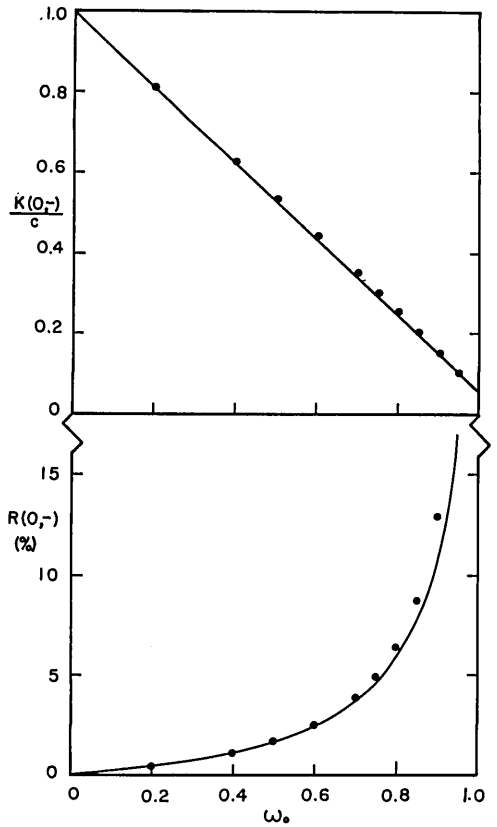

Fig. 7. Comparison of $K(0, -)/c$ and $R(0, -)$ computed from Eq. (12) and (13) (lines) with Monte Carlo computations (points) for phase function B in the sun case.

Conclusions

The apparent optical properties of a flat homogeneous ocean have been computed from the inherent optical properties for realistic scattering phase functions by a Monte Carlo technique that includes all orders of multiple scattering. The results of more than 125 separate cases considered have been analyzed to find general relationships between the inherent and apparent optical properties. These relationships can be used with measurements of $H(z, \pm)$ to determine the absorption and scattering coefficients as well as the forward and backscattering coefficients if c is also measured and to estimate the absorption coefficient in the absence of c. Since ω_0 and B are the important parameters in ocean color remote sensing work, we encourage the use of these relationships and hence simultaneous measurements of c and $H(z, \pm)$ to determine these quantities as a function of wavelength and the concentration of suspended sediments, phytoplankton, dissolved organics, etc.

It is found that the combination $K(\tau, -)/cD_0(\tau, -)$ appears to be independent of the incident radiance distribution, hence it is a quasi-inherent optical property. Also, $R(\tau, -)$ and $D(\tau, -) - D_0(\tau, -)$ are only weak functions of the incident radiance distribution. It is remarkable that for phase functions characteristic of sea water, the apparent optical properties depend on $P(\theta)$ only through the backscattering probability. This of course implies that measurements of $\beta(\theta)$ made over angular ranges not sufficient to determine B are essentially useless to the study of radiative transfer in the oceans.

Contribution 1811 University of Miami Rosenstiel School of Marine and Atmospheric Sciences. This work received support from the Office of Naval Research contract N000-14-67-A-0201-0013 Sub. 5.

Appendix A. Validity of the Quasi-Single-Scattering Approximation

In this Appendix we compare the predictions of the quasi-single-scattering approximation given in Eqs. (12) through (15) with the full multiple scattering Monte Carlo results. For this purpose only phase function B is used with collimated incident irradiance from the zenith. Figure 7 compares $K(0, -)/c$ and $R(0, -)$ (solid lines) with the computation from Eqs. (12) and (13) respectively. Clearly Eq. (12) gives a good approximation to $K(0, -)/c$ for all $\omega_0 < 0.95$, while Eq. (13) reproduces $R(0, -)$ very well for $\omega_0 < 0.6$. In Fig. 8 we compare $D(0, -)$ and $D(0, +)$ given by Eqs. (14) and (15) (solid lines) with the Monte Carlo calculations. Equation (14) is seen to produce acceptable values of $D(0, -)$ for $\omega_0 \lesssim 0.8$. Equation (15) predicts that $D(0, +)$ is independent of ω_0, and for phase function B should have a value of 1.923. The Monte Carlo values range between 1.85 and about 2.00, so to within about 4% Eq. (15) is also seen to be valid. Clearly however there is a weak dependence of $D(0, +)$ on ω_0 which, if we ignore $\omega_0 = 0.2$ and 0.4, could be approximated by adding a term proportional to X to Eq. (15). As mentioned in the text, Fig. 8 clearly shows that $D(0, +)/D(0, -) \approx 2$.

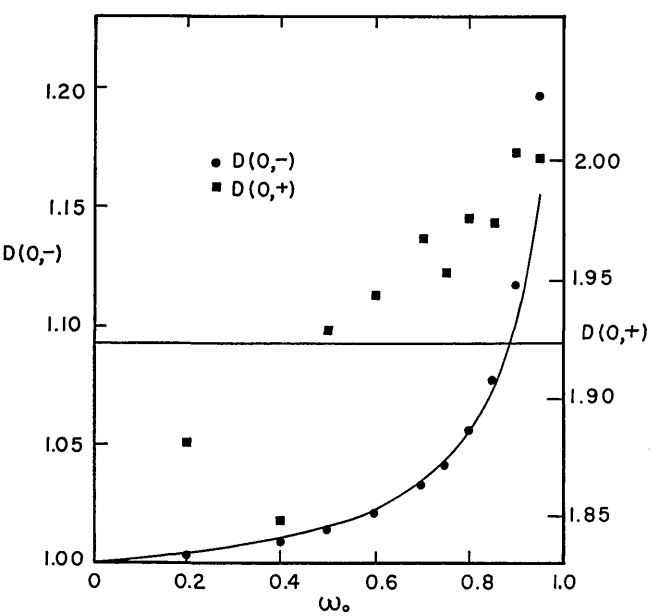

Fig. 8. Comparison of $D(0, \pm)$ computed from Eqs. (14) and (15) (lines) with Monte Carlo computations (points) for phase function B in the sun case.

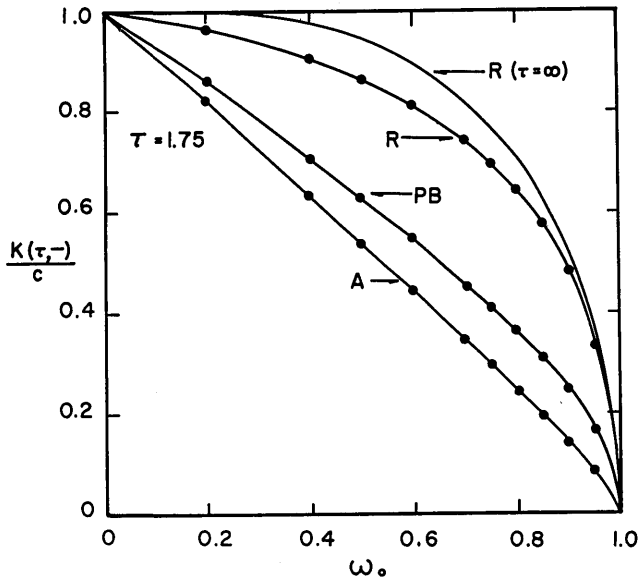

Fig. 9. Comparison of computations of $K(\tau, -)$ for Rayleigh scattering R and phase functions A (most forward scattering) and PB (least forward scattering) used in this study.

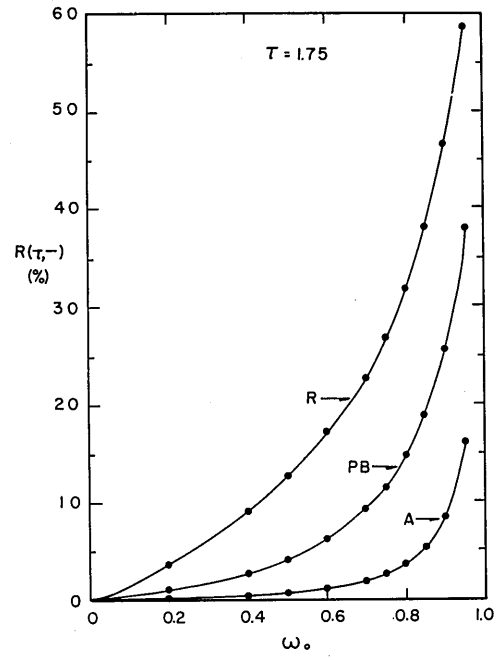

Fig. 10. Comparison of computations of $R(\tau, -)$ for Rayleigh scattering R and phase functions A and PB used in this study.

Appendix B. Rayleigh Scattering

If the oceans were completely uncontaminated by particulate matter, they would scatter light according to the Rayleigh phase function *(R)*,

$$P(\theta) = 3(1 + \cos^2\theta)/16\pi.$$

The results of simulations with this phase function were not discussed in the text, because they differ considerably from those obtained using phase functions strongly peaked in the forward direction. For example, Fig. 9, which gives $K(\tau, -)/c$ as a function of ω_0 for phase functions R, PB, and A at $\tau = 1.75$, shows that for $\omega_0 \lesssim 0.7$, $K(\tau, -)$ is a much weaker function of ω_0 for R than for A or PB. It should be noted that of the phase functions used in this study, A has the greatest amount of forward scattering, while PB has the least forward scattering. Since it is unlikely that surface waters will have a value of F less than that for PB, data for clear oceans should all fall below the PB curve in Fig. 9, while data for turbid waters may even fall slightly below the A curve. For water free of particles, it is unlikely that ω_0 is ever $\gtrsim 0.2$, so such an ocean would exhibit $K(\tau, -) \approx c$. We have also computed $K(\tau, -)/c$ as $\tau \to \infty$ (the asymptotic value) for R using the method of Herman and Lenoble,[17] and this is also shown in Fig. 9. Clearly, as $\tau \to \infty$, $K(\tau, -) \to c$ for pure water.

Figure 10 gives the computed values of $R(\tau, -)$ at $\tau = 1.75$ for these three phase functions. Rayleigh scattering is seen to lead to higher values of $R(\tau, -)$ for a given ω_0 than the phase functions used in this study. This is due to the large value of backscattering ($B = 0.5$) compared to the oceanic phase functions. Again, data for clear oceans should fall between the PB and A curves, and some turbid waters may even have reflectances that fall below the A curve. It is interesting, however, to note that the reflectance of an ocean composed only of pure water would be of the same order of magnitude as that in real oceans at the wavelengths of maximum ω_0. $R(\tau, -)$ was also computed for Rayleigh scattering in the limit as $\tau \to \infty$ but is not shown on Fig. 10 since it is only slightly above the $\tau = 1.75$ curve.

References

1. T. J. Petzold, *Volume Scattering Functions for Selected Waters* (Scripps Institution of Oceanography, University of California at San Diego, 1972), SIO Ref. 72–78.
2. N. G. Jerlov, *Optical Oceanography* (Elsevier, Amsterdam, 1968).
3. J. E. Tyler, and R. C. Smith, *Measurements of Spectral Irradiance Underwater* (Gordon and Breach, New York, 1970).
4. R. W. Preisendorfer, U.G.G.I., Monogr. **10,** 11 (1961).
5. J. E. Tyler, R. C. Smith, and W. H. Wilson, Jr., J. Opt. Soc. Am. **62,** 83 (1972).
6. H. R. Gordon, Appl. Opt. **12,** 2803 (1973).
7. In this work μ is always $\cos\theta$, and unprimed μ's refer to rays beneath the sea surface, while primed μ's refer to rays above the sea surface.
8. H. R. Gordon and O. B. Brown, Appl. Opt. **12,** 1544 (1973).
9. G. Kullenberg, Deep Sea Res. **15,** 423 (1968).
10. G. N. Plass, G. W. Kattawar, and J. Binstock, J. Quant. Spectrosc. Radiat. Transfer. **13,** 1081 (1973).
11. G. N. Plass, G. W. Kattawar, and F. E. Catchings, Appl. Opt. **12,** 314 (1973).
12. L. Prieur and A. Morel, Cahiers Ocean **23,** 35 (1971).
13. G. F. Beardsley, Jr., and J. R. V. Zaneveld, J. Opt. Soc. Am. **59,** 373 (1969).
14. C. Cox and W. Munk, J. Opt. Soc. Am. **44,** 838 (1954).
15. G. Maul and H. R. Gordon. *Relationships Between ERTS Radiances and Gradients across Oceanic Fronts,* presented at the Third ERTS-1 Principal Investigator's Symposium.
16. H. R. Gordon and W. R. McCluney, Appl. Opt. **14,** 413 (1975).
17. M. Herman and J. Lenoble, J. Quant. Spectrosc. Radiat. Transfer **8,** 355 (1968).